

Bucknell University

Bucknell Digital Commons

Faculty Journal Articles

Faculty Scholarship

1-2018

Energy conserving thermoregulatory patterns and lower disease severity in a bat resistant to the impacts of white-nose syndrome

Marianne S. Moore
Bucknell University

Kenneth A. Field
Bucknell University

Melissa J. Behr
University of Wisconsin, Madison

Gregory G. Turner
Pennsylvania Game Commission

Morgan E. Furze
Bucknell University

See next page for additional authors

Follow this and additional works at: https://digitalcommons.bucknell.edu/fac_journ



Part of the [Biology Commons](#), and the [Ecology and Evolutionary Biology Commons](#)

Recommended Citation


Moore, Marianne S.; Field, Kenneth A.; Behr, Melissa J.; Turner, Gregory G.; Furze, Morgan E.; Stern, Daniel WF; Allegra, Paul R.; Bouboulis, Sarah A.; Musante, Chelsey Diana; Vodzak, Megan E.; Biron, Matthew E.; Meierhofer, Melissa B.; Frick, Winifred F.; Foster, Jeffrey T.; Howell, Daryl; Kath, Joseph A.; Kurta, Allen; Nordquist, Gerda; Johnson, Joseph S.; Lilley, Thomas M.; Barrett, Benjamin W.; and Reeder, DeeAnn M.. "Energy conserving thermoregulatory patterns and lower disease severity in a bat resistant to the impacts of white-nose syndrome." *Journal of Comparative Physiology B* (2018) : 163-176.

This Article is brought to you for free and open access by the Faculty Scholarship at Bucknell Digital Commons. It has been accepted for inclusion in Faculty Journal Articles by an authorized administrator of Bucknell Digital Commons. For more information, please contact dcadmin@bucknell.edu.

Authors

Marianne S. Moore, Kenneth A. Field, Melissa J. Behr, Gregory G. Turner, Morgan E. Furze, Daniel WF Stern, Paul R. Allegra, Sarah A. Bouboulis, Chelsey Diana Musante, Megan E. Vodzak, Matthew E. Biron, Melissa B. Meierhofer, Winifred F. Frick, Jeffrey T. Foster, Daryl Howell, Joseph A. Kath, Allen Kurta, Gerda Nordquist, Joseph S. Johnson, Thomas M. Lilley, Benjamin W. Barrett, and DeeAnn M. Reeder

Energy conserving thermoregulatory patterns and lower disease severity in a bat resistant to the impacts of white-nose syndrome

Marianne S. Moore^{1,2} · Kenneth A. Field¹ · Melissa J. Behr³ · Gregory G. Turner⁴ · Morgan E. Furze¹ · Daniel W. F. Stern¹ · Paul R. Allegra¹ · Sarah A. Bouboulis¹ · Chelsey D. Musante¹ · Megan E. Vodzak¹ · Matthew E. Biron¹ · Melissa B. Meierhofer¹ · Winifred F. Frick⁵ · Jeffrey T. Foster^{6,7} · Daryl Howell⁸ · Joseph A. Kath⁹ · Allen Kurta¹⁰ · Gerda Nordquist¹¹ · Joseph S. Johnson^{1,12} · Thomas M. Lilley¹ · Benjamin W. Barrett¹ · DeeAnn M. Reeder¹ 

Received: 20 September 2016 / Revised: 13 May 2017 / Accepted: 17 May 2017
© Springer-Verlag Berlin Heidelberg 2017

Abstract The devastating bat fungal disease, white-nose syndrome (WNS), does not appear to affect all species equally. To experimentally determine susceptibility differences between species, we exposed hibernating naïve little brown myotis (*Myotis lucifugus*) and big brown bats (*Eptesicus fuscus*) to the fungus that causes WNS, *Pseudogymnoascus destructans* (*Pd*). After hibernating under identical conditions, *Pd* lesions were significantly more prevalent and more severe in little brown myotis. This species difference in pathology correlates with susceptibility to WNS in the wild and suggests that survival is related to different host physiological responses. We observed another fungal infection, associated with neutrophilic inflammation, that

was equally present in all bats. This suggests that both species are capable of generating a response to cold tolerant fungi and that *Pd* may have evolved mechanisms for evading host responses that are effective in at least some bat species. These host–pathogen interactions are likely mediated not just by host physiological responses, but also by host behavior. *Pd*-exposed big brown bats, the less affected species, spent more time in torpor than did control animals, while little brown myotis did not exhibit this change. This differential thermoregulatory response to *Pd* infection by big brown bat hosts may allow for a more effective (or less pathological) immune response to tissue invasion.

Keywords White-nose syndrome · *Pseudogymnoascus destructans* · *Myotis lucifugus* · *Eptesicus fuscus* · Fungal pathogen · Species differences

Communicated by H.V. Carey.

Electronic supplementary material The online version of this article (doi:10.1007/s00360-017-1109-2) contains supplementary material, which is available to authorized users.

✉ DeeAnn M. Reeder
dreeder@bucknell.edu

¹ Department of Biology, Bucknell University, Lewisburg, PA 17837, USA

² Present Address: College of Integrative Sciences and Arts, Arizona State University at the Polytechnic Campus, Mesa, AZ 85212, USA

³ Department of Pathobiological Sciences, School of Veterinary Medicine, University of Wisconsin-Madison, 2015 Linden Drive, Madison, WI 53706, USA

⁴ Pennsylvania Game Commission, Harrisburg, PA 17110, USA

⁵ Department of Ecology and Evolutionary Biology, University of California Santa Cruz, Santa Cruz, CA 95064, USA

⁶ Center for Microbial Genetics and Genomics, Northern Arizona University, Flagstaff, AZ 86011, USA

⁷ Present Address: Department of Molecular, Cellular and Biomedical Science, University of New Hampshire, Durham, NH 03824, USA

⁸ Iowa Department of Natural Resources, Des Moines, IA 50319-0034, USA

⁹ Illinois Department of Natural Resources, Springfield, IL 62702, USA

¹⁰ Department of Biology, Eastern Michigan University, Ypsilanti, MI 48197, USA

¹¹ Minnesota Department of Natural Resources, St. Paul, MN 55155-4015, USA

¹² Present Address: Department of Biological Sciences, Ohio University, Athens, USA

Introduction

The emergence of pathogens that cause disease and mortality in multiple wildlife species is on the rise, affecting hosts in a variety of taxonomic groups (Dobson and Foutopoulos 2001; Tompkins et al. 2015). Major decreases in the global biodiversity of host species (Skerratt et al. 2007) and/or massive population declines in one or several host species have occurred (Frick et al. 2010; Thogmartin et al. 2012), driving the need for greater understanding of variable susceptibility among host species. One multi-host disease, white-nose syndrome (WNS), is causing one of the most precipitous declines of wild mammals ever recorded, with an overall tenfold decrease in the abundance of bats at hibernacula in eastern North America (Frick et al. 2015) and the predicted regional or range-wide extinction of at least two North American species (Frick et al. 2010; Thogmartin et al. 2012, 2013). The United States Fish and Wildlife Service estimated that >5.5 million individuals died from WNS between the emergence of this disease in 2006 and January 2012 (USFWS 2012) and multiple host species are impacted, but to varying degrees (Turner et al. 2011; Langwig et al. 2012). DNA from the pathogen has been identified on 12 North American species of bat from six genera and seven of these species have been documented with skin lesions diagnostic of WNS, whereas no skin lesions have been observed on the remaining five species (Bleher et al. 2009; Gargas et al. 2009; Chaturvedi et al. 2010; Bernard et al. 2015; US FWS: <https://www.whitenosesyndrome.org/about/bats-affected-wns/>). DNA from the pathogen has also been isolated from multiple species of bat throughout Europe and in Asia (Puechmaile et al. 2011; Hoyt et al. 2016) and lesions characteristic of WNS have been identified in some of these species (Pikula et al. 2011; Zukal et al. 2014; Hoyt et al. 2016). However, there have been no reports of mortality in Europe or Asia and a novel introduction of the pathogen in North America is supported by results from experimental inoculations and genetic analyses, both using European and North American fungal isolates (Warnecke et al. 2012; Leopardi et al. 2015).

A psychrophilic fungus (*Pseudogymnoascus destructans* Gargas et al. 2009, hereafter *Pd*) has been identified as the causative agent of WNS (Gargas et al. 2009; Lorch et al. 2011). *Pd* invades the epidermis and dermis of hibernating bats causing distinctive cupping erosions that allow diagnosis and quantification of disease severity (Meteyer et al. 2009; Reeder et al. 2012). Fungal hyphae can invade hair follicles, sebaceous glands, and apocrine glands, and destroy connective tissues, causing widespread structural damage. The little brown myotis (*Myotis lucifugus*) is one of the most highly affected species, with declines in some populations of up to 91% (Frick et al. 2010, 2015; Turner et al. 2011). This species has been the focus of most WNS

research to date (Reeder et al. 2016). In this species, WNS is associated with a number of abnormalities, including: premature reductions in body condition (Bleher et al. 2009; Meteyer et al. 2009; Courtin et al. 2010; Moore et al. 2011; Storm and Boyles 2011; Warnecke et al. 2012), altered thermoregulation leading to increased frequency of arousal from torpor (Reeder et al. 2012; Warnecke et al. 2012), behavioural changes during arousals (Brownlee-Bouboulis and Reeder 2013; Johnson et al. 2014; Wilcox et al. 2014), increased fat depletion and altered blood physiology (Cryan et al. 2010; Warnecke et al. 2013; Verant et al. 2014), wing damage in active-season, non-hibernating bats (Reichard and Kunz 2009; Francl et al. 2011; Fuller et al. 2011), altered blood-based immune parameters (Moore et al. 2011, 2013), and dramatic shifts in the expression of inflammatory, wound healing, and metabolic genes (Field et al. 2015).

Within species known to develop cutaneous lesions and experience mortality, population-level impacts vary (Langwig et al. 2012). Declines in hibernating populations range from as low as 12% to as high as 98% during the 5 years directly following emergence of WNS (2006–2011; Turner et al. 2011). Although there have been noted declines in some hibernating populations of big brown bats (*Eptesicus fuscus*), across multiple populations, there has not been a significant decline (Langwig et al. 2012). In fact, recent field surveys suggest that big brown bats do not die from WNS despite hibernating in the same sites as infected little brown myotis (Frank et al. 2014). Multiple host traits may contribute to the observed differential impacts of WNS across species (Reeder and Moore 2013; Hayman et al. 2016). These traits may include body size, length of hibernation period, attributes of hibernacula and microclimate selection (Wilder et al. 2011; Halsall et al. 2012; Johnson et al. 2014; Grieneisen et al. 2015), population size and social structure (Wilder et al. 2011; Langwig et al. 2012; Frick et al. 2015), rates of evaporative water loss (Cryan et al. 2010; Willis et al. 2011; Warnecke et al. 2013), sebaceous lipid composition (Frank et al. 2016), and microbial communities on skin surfaces (Hoyt et al. 2015; Avena et al. 2016). When the fungus does successfully infect the host, immune defences likely affect the outcome of infection (Romani 2011; Johnson et al. 2015; Field et al. 2015).

To date, no study has experimentally compared the development of WNS infections or described variation in any physiological responses among different bat species exposed to *Pd* (Hayman et al. 2016). We performed experimental infection trials in little brown myotis and the less affected big brown bat and measured interspecies variation in prevalence and severity of WNS. We focused on these two species because of their differential population-level responses to WNS. Thus, understanding variation in how big brown bats and little brown myotis respond to *Pd*

invasion may help to construct models of responses that are effective vs. maladaptive. Knowledge of responses specific to big brown bats and little brown myotis may provide useful information applicable to species with similar population-level effects, life history traits, and physiological characteristics. We tested the hypothesis that, when exposed to the same dose of *Pd* conidia and housed under identical conditions, the two species would differ in the manifestation of cutaneous *Pd* infection and in their response to infection. We controlled for species differences in microclimate preferences during hibernation, which are known to affect proliferation of *Pd* (Verant et al. 2012) and mortality in *Pd*-exposed little brown myotis (Langwig et al. 2012; Johnson et al. 2014; Grieneisen et al. 2015).

Materials and methods

Ethics

Capture, handling, and sample collection protocols for this study were reviewed and approved by the Bucknell University IACUC (protocol #DMR-12), and the US Fish and Wildlife Service Disinfection Protocol for Bat Studies was used during all collections. In the states of Illinois and Iowa, research collections were conducted by state wildlife officials and on non-endangered bats; thus, numbered permits were not required or issued. In Michigan and Minnesota, research was conducted under Scientific Collector's Permits #SC1448 to DMR and #201174 to DMR, respectively.

Animal collection and transportation

Big brown bats and little brown myotis were hand collected from five hibernacula during late fall 2011: two mines in Dickinson County, MI on 5 November 2011; one mine in St. Louis County, MN on 16 November 2011; one mine in LaSalle County, IL on 17 November 2011; and one cave in Jackson County, IA on 17 November 2011. Hibernacula were selected to acquire sufficient numbers of presumably naïve individuals from within a geographically limited area while limiting the removal of large numbers of bats from any one site. Hibernacula that fit these criteria were located within a geographic area that spanned a range of mean annual surface temperatures (0–10°C), which are a good predictor of cave microclimate. Sample sizes were based upon our previous experiences studying bat physiology, balancing the need to minimize removal of *Pd* unaffected bats from the wild (Reeder et al. 2016). At the capture sites, bats were immediately swabbed on the left forearm and the sample was stored for qPCR analysis to determine presence or absence of *Pd* in the field. Bats were also visually

examined for evidence of fungal infection and none exhibited visual evidence of *Pd* infection in any of the hibernacula. Bats were then individually placed in cloth bags for transport from their hibernaculum. Researchers changed gloves between each bat to avoid cross-contamination. Outside hibernacula, all bats were weighed, uniquely marked with a 2.9 mm aluminium alloy band (Porzana Ltd.) on the forearm, and then transported to Bucknell University at 4°C (transport time 26–55 h) using methods described in Johnson et al. (2015).

Animal housing

We housed all bats in one of four environmental chambers (Percival model # I36VLC8) with conditions set to 4°C and 95% relative humidity. One chamber (P1) maintained 85% RH regardless of the set point. Two chambers were designated for control bats and two for *Pd*-exposed bats. We minimized and equalized disturbance to bats during the experiment by opening chamber doors only for inoculations or for sample collections and by housing bats to be sampled on different weeks post-infection in separate cages. Big brown bats and little brown myotis were housed in separate cages. Bats were provided with water throughout the experiment. Before inoculation with *Pd*, bats were again weighed, had forearm length measured and reproductive stage, relative age (i.e., juvenile vs. adult based on enlargement of testes and distension of cauda epididymides in males and development of nipples in females) and sex recorded. Each individual was equipped with a temperature-sensitive data logger to record skin temperature throughout the experiment and was photographed with UV light. To control for the potential physiological variation between bats as a function of differences in microclimate across capture sites, differences in starting mass, and differences in sex, we randomly assigned bats to a treatment group while also comprehensively balancing assignments according to sex, mass, and capture site. Bats were weighed again before euthanasia to document changes in body condition, which was expressed as \log_{10} -body mass divided by \log_{10} -forearm length. Data for all animals, including group assignment, are available in the supplement (Supplemental Table 1).

Inoculations with *Pseudogymnoascus destructans*

Inoculations with *Pd* or carrier alone were conducted on 19 (controls) and 21 (*Pd*) December 2012. 350,000 *Pd* conidia suspended in 20- μ L phosphate buffered saline (PBS) with 0.5% TWEEN-20 was dispensed onto the ventral side of the left wing membrane of each exposed bat near the metacarpals. This dose is within the range of that used in other successful infection studies (Lorch et al. 2011; Johnson et al. 2014). This solution was gently spread

from the anterior surface to posterior surface of the membrane using the pipette tip. For controls, 20 μ L PBS with 0.5% TWEEN-20 was dispensed in the same manner. For each group, treatment wings were gently folded, so that dispensed liquid was on the inside surface and bats were immediately returned to the cages used for housing during the experiment.

Wing tissue collection

At 3, 7, and 13-weeks post-inoculation, we sampled bats of each species in control and experimental groups. Individual bats were removed from the cage and immediately swabbed on the left forearm for qPCR identification and quantification of *Pd* on wing membranes and we recorded body mass. We euthanized bats by isoflurane overdose followed by decapitation. The left wing of each bat was removed and stored on ice for overnight shipment to MJB for histological analysis.

Temperature tracking

Temperature-sensitive dataloggers were programmed to record skin temperature (T_{sk}) every 20 min and were attached to the back of bats using standard methods (Willis and Brigham 2003). Loggers (Thermochron DS1922L iButtons; Maxim Integrated Products, Inc., California, USA) were modified by the authors as previously described (Reeder et al. 2012). Due to technical failures, we only present body temperature data from the 13-week group, monitored from December 20, 2011 to February 10, 2012. We used the minimum T_{sk} value of each bat to determine when it was torpid and aroused, because bats were maintained at a constant temperature for the duration of the experiment and rested within 0.5°C of the minimum T_{sk} for >99% of readings. We considered bats to be torpid when T_{sk} was within 10°C of the minimum T_{sk} , and considered bats to be aroused when T_{sk} was >10°C above the minimum T_{sk} for >1 reading.

Histology

The left wing was cut along the leg and body, and the humerus was severed. Wing membranes were removed from the bones of the arm and digits and rolled onto 1.0–1.5-cm-diameter paraffin wax “logs.” Two logs were made from each little brown myotis and three from big brown bats. The logs were fixed in 10% neutral buffered formalin for at least 24 h. Each log was cut into three pieces (“wing rolls”), which were processed into paraffin blocks overnight in a Tissue-Tek VIP processor (Sakura Finetek). The rolls were embedded in paraffin blocks, sectioned width of 3 microns, stained with periodic acid-Schiff with a

hematoxylin counterstain (Meteyer et al. 2009), and examined for number of *Pd* lesions based on the published diagnostic criteria for WNS (Meteyer et al. 2012), number of unidentified fungal foci (i.e. fungal invasion that did not fit the WNS criteria), number of inflammatory foci, and the total number of wing rolls affected by each type of foci. Proportion of wing area affected by each type of foci was estimated by dividing the number of affected wing rolls by the total number of wing rolls examined. To control for differences in total wing area analysed between species, we divided the total number of *Pd* lesions, unidentified fungal foci, and inflammatory foci by the number of rolls examined. We used values standardized to wing area for our statistical analyses, but present absolute numbers of *Pd* lesions, unidentified fungal foci, and inflammatory foci in figures and the text.

QPCR detection and quantification of *Pd*

Real-time PCR was used to verify the presence of *Pd* DNA and estimate fungal load on each bat (Muller et al. 2013). Quantification of fungal DNA was determined based on the cycle threshold (Ct) with a Ct cutoff of 40 cycles, as in Langwig et al. (2015).

Ultraviolet image capture and analysis

The left wing of each bat sampled at the 13-week time point was photographed prior to freezing using transillumination with long-wave UV light (Turner et al. 2014). Digital images were analysed blindly using Cellprofiler 2.1.0 (Broad Institute). After selecting the green (or red and green) RGB channel, a Wacom Intuos 5 tablet was used to manually trace fluorescent regions of the wing, which indicate infection, as well as the entire border that was visible and in focus within the image. Results are presented as the ratio of the fluorescing area to the total wing area.

Statistical analysis

We categorized groups of bats based on species, treatment (*Pd*-exposed or control), and week post-exposure. After standardizing lesions to total wing area examined, we compared prevalence of *Pd* lesions, skin inflammation and an additional fungal infection discovered during histology between the two species using Fisher’s exact test. Within each species, we used Pearson’s χ^2 to test for differences in prevalence of *Pd* lesions, skin inflammation, and the unidentified fungal infection over the time course of the experiment. We compared severity of *Pd* lesions between species and tested for the change in severity of *Pd* lesions over time. We compared body condition data between *Pd*-exposed and control bats within each species at each time

post-exposure and made three-way comparisons to test for changes in response variables over time. Differences in thermoregulatory measures between Pd-exposed and control bats of each species were described for bats sampled only in week 13.

For each comparison, outcome variables (i.e. Pd lesion severity, severity of tissue inflammation, severity of the unidentified fungal infection discovered during histology, Pd load based on qPCR, wing fluorescence using UV analysis, thermoregulation parameters, and body condition) were examined for normality and homogeneity of variance using Shapiro-Wilks tests and Levene's test. For two-way comparisons, we used student *t* tests for normally distributed data sets with equal variances and non-parametric Mann–Whitney *U* tests for non-normally distributed data with equal variances. We used unequal variance *t* tests on data sets with normal distributions but unequal variances, and ranked unequal variance *t* tests on data sets with non-normal distributions and unequal variances. For three-way comparisons, we used ANOVAs on normally distributed data sets, Kruskal–Wallis on data sets with non-normal distributions, Welch's ANOVA on data sets with normal distribution but unequal variances, and ranked Welch's ANOVA on data sets with non-normal distributions and unequal variances. We tested for correlations between Pd lesions, skin inflammation, body condition, severity of the additional fungal infection, Pd load based on qPCR, and wing fluorescence using Spearman's ρ . For thermoregulatory (four two-way tests) and body condition (six two-way tests) data, we used false discovery rates (FDR) to control for the error introduced by testing multiple hypotheses (Benjamini and Hochberg 1995). Non-normal distributions and small sample sizes prevented us from controlling for other variables, such as capture site, body mass and sex, that may have affected the outcomes measured. However, our balanced and randomized assignment of bats to treatment groups should have minimized the effects of these variables on our findings. Statistical analyses were performed using SPSS version 21.0.0.0 (2012; IBM, Armonk, New York). The R package ggplot2 was used to generate all figures (Wickham 2009). Our data are available in the Dryad Repository at: <http://dx.doi.org/10.5061/dryad.612dg>.

Results

Histological evidence of differential severity in cutaneous Pd infection between little brown myotis and big brown bats

Forty-seven of sixty-six (71%) bats exposed to Pd developed epidermal cupping erosions diagnostic of WNS (herein referred to as Pd lesions; Meteyer et al. 2009),

whereas none of 66 control bats showed histological evidence of Pd infection. Significantly more Pd-exposed little brown myotis developed Pd lesions than did Pd-exposed big brown bats (Fig. 1a, $n = 18/37$ exposed vs. $n = 5/29$ exposed, Fisher's exact test $p = 0.022$). For bats with Pd lesions, individual little brown myotis developed more Pd lesions than big brown bats after standardizing Pd lesion count to wing area (Fig. 1b; range

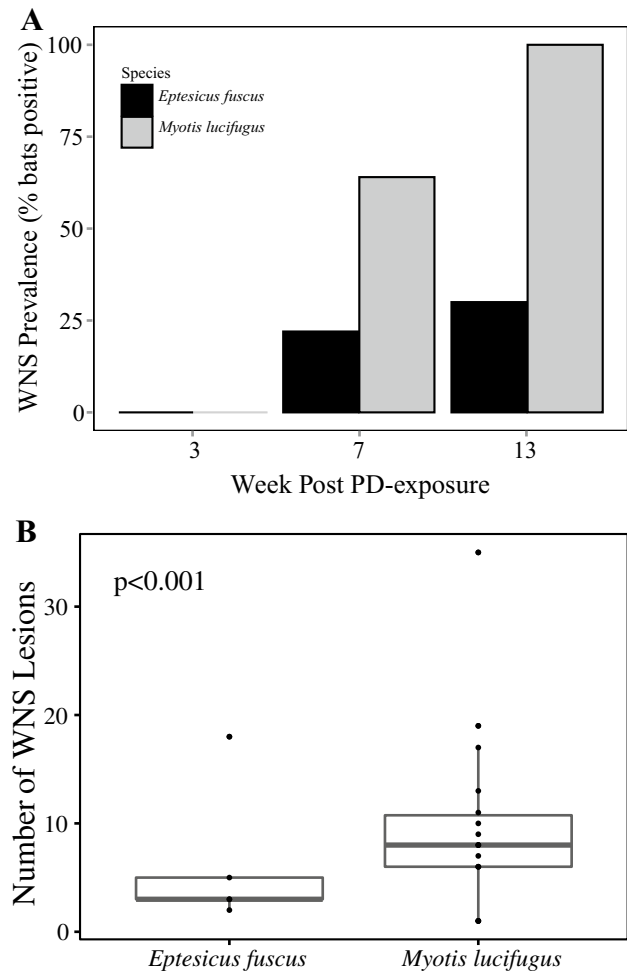


Fig. 1 Big brown bats (*Eptesicus fuscus*) developed fewer and less severe infections than little brown myotis (*Myotis lucifugus*). **a** Prevalence, as percentage of bats in each group, of skins lesions diagnostic of white-nose syndrome (WNS) in little brown myotis and big brown bats across the three sampling periods for histological analysis post-exposure to *Pseudogymnoascus destructans* (Pd). Significantly more Pd-exposed little brown myotis developed Pd lesions than did Pd-exposed big brown bats (Fisher's exact test $p = 0.022$). **b** Number of Pd lesions observed in each species. After standardizing lesion counts to wing area, which differs between the two species, significantly more Pd lesions were observed in little brown myotis compared with big brown bats (unequal variance $t = 4.34$, $df = 114.13$, $p < 0.001$). Absolute counts of Pd lesions are presented using box plots indicating medians in thick lines and first and third quartiles at bottom and top of boxes, respectively. Whiskers indicate values within 1.5 \times the interquartile range

of 1–35 lesions per wing in little brown myotis, mean rank = 12.78, mean = 2.2 vs. range of 1–8 lesions per wing in big brown bats, mean rank = 9.84, mean = 0.55; unequal variance $t = 4.34$, $df = 114.13$, $p < 0.001$). Furthermore, little brown myotis exhibited distinct *Pd* lesions, whereas big brown bats had lesions that fit the diagnostic criteria for WNS, but that were less well-defined, with more confluent foci of epidermal invasion. The presence of *Pd* lesions also increased significantly across weeks post-exposure in little brown myotis (Pearson's $\chi^2 = 13.64$, $p = 0.001$) but not in big brown bats (Pearson's $\chi^2 = 3.07$, $p = 0.22$). Among bats exposed to *Pd*, no *Pd* lesions were observed in either species sampled at week 3; 2 of 9 and 3 of 10 big brown bats showed *Pd* lesions at 7 and 13 weeks respectively; and 9 of 14 and 9 of 9 little brown myotis showed *Pd* lesions at weeks 7 and 13 respectively (Fig. 1a). It is important to note that the chamber (P1) housing bats euthanized at 3-weeks post-exposure maintained 85% RH despite a 95% RH setting. Although optimal relative humidity is unknown for *Pd*, it is possible that prevalence may have been different (presumably higher) in this group if 95% RH had been maintained.

Pd DNA and UV quantification of infection

At the time of euthanasia, 46 (69.7%) *Pd*-exposed bats of both species were qPCR positive for *Pd* and 14 (21.3%) *Pd*-exposed bats were qPCR negative (6 were not tested). Of the 46 bats positive for *Pd* DNA, 27 were little brown myotis and 19 were big brown bats. Three of the *Pd*-exposed bats negative for *Pd* DNA based on qPCR had diagnostic *Pd* lesions. We also discovered that five big brown bats (two included in the control group, three included in the *Pd*-exposed group) were field positive (i.e., positive at the time of collection from the wild). However, the two field positive big brown bats included in our control group were qPCR negative for *Pd* at the time of euthanasia. In addition, in our control group, four other bats (one little brown myotis and three big brown bats) were qPCR positive for *Pd* (at trace amounts) at the time of euthanasia, but none of these were field positive and none showed histological evidence of *Pd* lesions. It is possible that these PCR positive control bats were false-positives due to contamination issues. Like the results from other studies, we rely primarily on histology results, the gold standard for WNS diagnosis (Meteyer et al. 2009). Given the trace amounts of *Pd* DNA detected and no evidence of *Pd* lesions in the four control bats, we retained data from these bats in our analyses comparing *Pd* load to *Pd* lesions, wing fluorescence, inflammatory foci, and unidentified fungal foci. Data from three of the four control bats positive for *Pd* at the time of euthanasia were also included in our analyses

of thermoregulatory behaviors, but only one of the five field positive big brown bats entered our analyses of torpor expression as a control (i.e., this bat was assigned to the control group and later found field positive using qPCR). Neither *Pd* load nor intensity of wing fluorescence differed between species (*Pd* load: little brown myotis mean rank = 21.87, mean = 2.1×10^{-004} ng, big brown bats mean rank = 26.87, mean = 4.0×10^{-005} ng, unequal variance $t = -1.30$, $df = 44.99$, $p = 0.20$; intensity of wing fluorescence: little brown myotis mean rank = 20.62, mean intensity = 0.02, big brown bat mean rank = 18.12, mean intensity = 0.01, Mann–Whitney $U = 155$, $p = 0.50$). *Pd* load did not differ across weeks post-exposure in big brown bats (Welch's ANOVA $F_{2,6.01} = 2.71$, $p = 0.15$) or in little brown myotis (Welch's ANOVA $F_{2,9.18} = 3.87$, $p = 0.06$).

In little brown myotis, *Pd* load was positively correlated with the number of *Pd* lesions, the number of unidentified fungal foci, and the number of inflammatory foci ($n = 27$, *Pd* lesions Spearman's $\rho = 0.56$, $p = 0.002$; unidentified fungal foci Spearman's $\rho = 0.60$, $p = 0.001$; inflammatory foci Spearman's $\rho = 0.49$, $p = 0.01$). However, *Pd* load did not correlate with wing fluorescence ($n = 19$, Spearman's $\rho = 0.09$, $p = 0.71$). In contrast, for big brown bats, *Pd* load did not correlate with number of *Pd* lesions, number of unidentified fungal foci, number of inflammatory foci, or wing fluorescence ($n = 19$, *Pd* lesions Spearman's $\rho = 0.07$, $p = 0.79$, unidentified fungal foci Spearman's $\rho = 0.27$, $p = 0.26$, inflammatory foci Spearman's $\rho = 0.23$, $p = 0.34$, wing fluorescence Spearman's $\rho = 0.39$, $p = 0.12$).

Thermoregulatory and body condition comparisons between *Pd*-exposed and control bats

Pd-exposed big brown bats exhibited an altered thermoregulatory response in the form of longer torpor bout durations (Fig. 2, *Pd*-exposed $n = 9$, mean rank = 12.78, mean duration = 14.7 days, control $n = 8$, mean rank = 4.75, mean duration = 7.6 days, Mann–Whitney $U = 2$, FDR corrected $p = 0.004$), whereas we found no significant thermoregulatory change in *Pd*-exposed little brown myotis compared with controls after correcting for multiple comparison testing (*Pd*-exposed $n = 8$, mean rank = 5.88, mean duration = 14.7 days, control $n = 8$, mean rank = 11.13, mean duration = 26.9 days, unequal variance $t = 2.59$, $p = 0.023$, FDR corrected $p = 0.09$). Arousal duration between torpor bouts did not differ between treatments in either species, nor did skin temperatures during torpor and interbout arousals. Hibernating bats lost weight between the date of inoculation and the date euthanized (both mass in g, and hence BMI, decreased over time; Table 1), but the decreases in BMI were not statistically significant. We did not detect any statistically significant differences in body condition between *Pd*-exposed and control bats of either

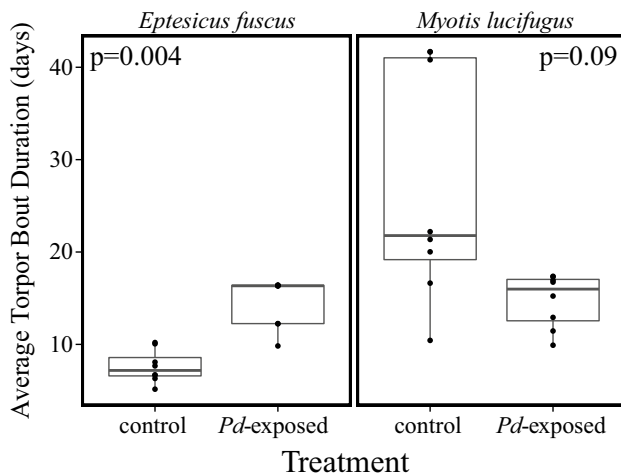


Fig. 2 *Pd*-exposed big brown bats (*Eptesicus fuscus*) spent more time in torpor compared with controls of the same species, whereas *Pd*-exposed little brown myotis (*Myotis lucifugus*) showed no difference in torpor expression compared with controls of the same species. Average time (days) spent in torpor in little brown myotis and big brown bats exposed to *Pseudogymnoascus destructans* (*Pd*) or sham-inoculated (controls). Compared with controls of the same species, *Pd*-exposed big brown bats exhibited longer torpor bout duration (Mann–Whitney $U=2$, FDR corrected $p=0.004$). In contrast, after controlling for testing multiple hypotheses, little brown myotis showed no significant change in torpor bout duration. Presented p values are corrected using the false discovery rate (FDR) method. Absolute torpor bout durations (in days) are presented using box plots indicating medians in thick lines and first and third quartiles at bottom and top of boxes respectively. Whiskers indicate values within $1.5\times$ the interquartile range

species across all times post-exposure. In little brown myotis, *Pd* load was positively correlated with skin temperature during torpor ($n=7$, Spearman's $\rho=0.81$, $p=0.027$), but not correlated with other measures of thermoregulation. Wing fluorescence was not correlated with any measure of thermoregulation in little brown myotis. In big brown bats, our measures of *Pd* load and wing fluorescence were not correlated with any thermoregulatory parameter. In both species, *Pd* load or wing fluorescence were not correlated with body condition at any time point, or change in body condition between *Pd*-inoculation and euthanasia. Complete test statistics for thermoregulatory and body condition parameters in *Pd*-exposed compared with control bats of both species are presented in Table 1.

Skin inflammatory responses

For the two species combined, 49 of 66 (74%) *Pd*-exposed and 50 of 64 (78%) control bats presented histological evidence of neutrophilic inflammation in wing tissues. A larger proportion of big brown bats exhibited inflammation compared with little brown myotis (little brown myotis $n=49$ of 73; big brown bats $n=50$ of 56; Fisher's exact test

$p=0.003$), but the proportion of individuals with inflammation within each species did not differ by *Pd* treatment, nor was there a difference between species in degree of inflammation (i.e., number of inflammatory foci or proportion of wing membrane exhibiting inflammation). Prevalence of inflammation increased in both species throughout the experiment (little brown myotis Welch's ANOVA $F_{2,70}=34.18$, $p<0.001$; big brown bats Welch's ANOVA $F_{2,53}=13.48$, $p<0.001$). In little brown myotis, the number of inflammatory foci was positively associated with number of *Pd* lesions (Fig. 3a, $n=37$, Pearson's $\rho=0.68$, $p<0.001$), whereas in big brown bats, this association was not significant (Fig. 3a, $n=28$, Pearson's $\rho=0.35$, $p=0.07$).

Forty-six of sixty-six (70%) *Pd*-exposed and 43 of 64 (67%) control bats across the two species showed histological evidence of a fungal infection that was not morphologically characteristic of WNS (Figs. 3b, 4). In contrast to *Pd* invasion, the fungus responsible for the infection (herein "unidentified fungal infection") produced mats along the wing surface with variable penetration into the epidermis and dermis. It did not cause lesions similar to those diagnostic of WNS (Fig. 4a, c). Prevalence of the unidentified fungal infection did not differ between *Pd*-exposed and unexposed bats within either species but the unidentified fungal infection was more prevalent in big brown bats than little brown myotis (42 of 73 little brown myotis were positive; 47 of 57 big brown bats were positive; Fisher's exact test $p=0.002$). There was no overall difference in the amount of the unidentified fungal infection (i.e., proportion wing affected and number of foci) between the species, and for big brown bats that had the unidentified fungal infection, severity did not differ by treatment (*Pd*-exposed vs. sham-inoculated).

In little brown myotis that had the unidentified fungal infection, *Pd*-exposed bats had more wing area affected by the unidentified fungus (*Pd*-exposed $n=37$, mean rank=41.57, mean=0.80, control $n=36$, mean rank=32.31, mean=0.49, $df=68.5$; unequal variance $t=2.01$ $p=0.049$) and more invasion foci (*Pd*-exposed $n=37$, mean rank=42.93, mean=261 foci, control $n=36$, mean rank=30.90, mean=20 foci, $df=63.29$, unequal variance $t=2.64$ $p=0.011$) compared with controls (sham-inoculated). Control little brown myotis (not exposed to *Pd*) that developed the unidentified fungal infection had relatively lower body condition at the time of capture in the wild compared with control little brown myotis that did not develop the unidentified fungal infection (unidentified fungal infection present $n=18$, mean initial body condition=0.58, unidentified fungal infection absent $n=17$, mean initial body condition=0.60, $df=33$, $t=-2.61$, $p=0.013$).

The presence of the unidentified fungal infection increased in frequency from week 3 to week 13 in both species (little

Table 1 Test statistics from comparisons of thermoregulatory behaviors and body condition measurements in (A) *Pd*-exposed and control big brown bats and (B) *Pd*-exposed and control little brown myotis

	Week post-exposure	Control, <i>n</i>	Mean	SD	Median	Mean rank	<i>Pd</i> -exposed, <i>n</i>	Mean	SD	Median	Mean rank	<i>df</i>	Test statistic	<i>p</i> value	FDR corrected <i>p</i> value	
A Big brown bats (<i>Eptesicus fuscus</i>)																
Torpor bout duration	13	8	7.6 days	1.8	7.2 days	4.75	9	14.7 days	2.6	16.3 days	12.78	na	M–W $U=2$	0.001*	0.004*	
Interbout arousal duration	13	8	2.3 h	0.03	2.0 h	na	9	2.8 h	0.02	2.6 h	na	15	$t=1.79$	0.093	0.19	
Average skin temperature during arousal	13	8	23.7 °C	1.3	24.1 °C	na	9	24.9 °C	1.9	25.1 °C	na	15	$t=1.46$	0.16	0.19	
Average skin temperature during torpor	13	8	6.5 °C	0.4	6.6 °C	10.69	9	6.4 °C	0.5	6.2 °C	7.5	na	M–W $U=22.5$	0.19	0.19	
Body condition at euthanasia	3	9	0.73	0.02	0.72	na	10	0.73	0.02	0.73	na	17	$t=0.78$	0.45	0.94	
	7	9	0.72	0.03	0.72	na	9	0.72	0.03	0.73	na	16	$t=0.08$	0.94	0.94	
	13	10	0.71	0.02	0.71	na	10	0.71	0.02	0.71	na	18	$t=-0.43$	0.67	0.94	
Change in body condition from inoculation to euthanasia	3	9	-0.02	0.00	-0.02	6.89	10	-0.02	0.01	-0.02	12.8	na	M–W $U=17$	0.022	0.13	
	7	9	-0.04	0.01	-0.04	na	9	-0.04	0.01	-0.04	na	11.98	u.v. $t=-0.09$	0.93	0.94	
	13	10	-0.04	0.02	-0.05	na	10	-0.04	0.01	-0.04	na	10.76	u.v. $t=0.69$	0.51	0.94	
Change in body mass from inoculation to euthanasia	3	9	-1.52 g	0.32	na	na	10	-1.36 g	1.03	na	na	na	na	na	na	
	7	9	-2.59 g	0.89	na	na	9	-2.56 g	0.37	na	na	na	na	na	na	
	13	10	-2.64 g	1.26	na	na	10	-2.32 g	0.40	na	na	na	na	na	na	
B Little brown myotis (<i>Myotis lucifugus</i>)																
Torpor bout duration	13	8	26.9 days	12.6	21.8 days	11.13	8	14.7 days	2.9	16.0 days	5.88	12.07	u.v. $t=-2.59$	0.023	0.09	
Interbout arousal duration	13	8	8.4 h	0.02	0.96 h	na	8	0.72 h	0.01	0.72 h	na	14	$t=-0.14$	0.89	0.89	
Average skin temperature during arousal	13	8	22.0 °C	1.1	22.0 °C	na	8	21.64 °C	1.3	21.8 °C	na	14	$t=-0.32$	0.76	0.89	
Average skin temperature during torpor	13	8	6.2 °C	0.3	6.2 °C	9.63	8	6.1 °C	0.1	6.1 °C	7.38		M–W $U=23$	0.34	0.68	

Table 1 (continued)

	Week post-exposure	Control, <i>n</i>	Mean	SD	Median	Mean rank	<i>Pd</i> -exposed, <i>n</i>	Mean	SD	Median	Mean rank	<i>df</i>	Test statistic	<i>p</i> value	FDR corrected <i>p</i> value
Body condition at euthanasia	3	11	0.53	0.03	0.53	na	14	0.54	0.03	0.54	na	23	$t=0.11$	0.91	0.91
	7	12	0.54	0.02	0.54	na	14	0.53	0.03	0.53	na	24	$t = -0.29$	0.77	0.91
	13	12	0.53	0.02	0.52	na	8	0.51	0.02	0.52	na	18	$t = -1.4$	0.18	0.29
Change in body condition from inoculation to euthanasia	3	11	-0.02	0.01	-0.03	na	14	-0.02	0.01	-0.02	na	23	$t=1.36$	0.19	0.29
	7	12	-0.01	0.02	-0.01	na	12	-0.02	0.01	-0.02	na	22	$t = -2.04$	0.054	0.24
	13	12	-0.02	0.02	-0.02	na	7	-0.03	0.01	-0.03	na	17	$t = -1.86$	0.08	0.24
Change in body mass from inoculation to euthanasia	3	12	-0.64 g	0.30	na	na	14	-0.48 g	0.26	na	na	na	na	na	na
	7	12	-0.24 g	0.42	na	na	12	-0.55 g	0.33	na	na	na	na	na	na
	13	12	-0.43 g	0.40	na	na	7	-0.76 g	0.40	na	na	na	na	na	na

Significant differences (*) were determined at $\alpha=0.05$ and corrected for multiple tests using the false discovery rate method

M-W *U* Mann-Whitney *U*, *u.v.* *t* unequal variance *t* test, *SD* standard deviation, *FDR* false discovery rate, *na* not applicable to the analysis used

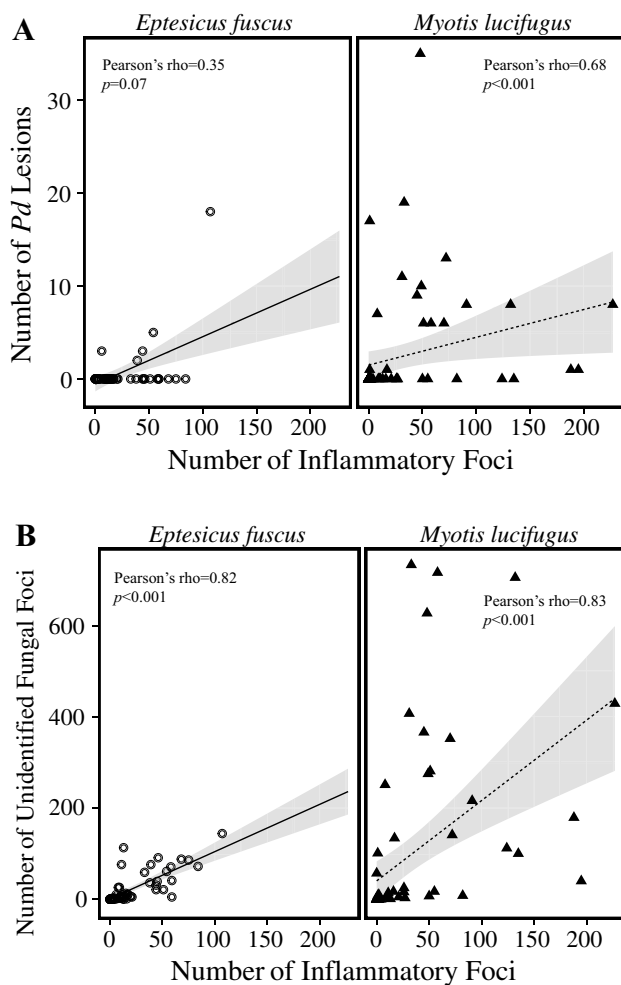


Fig. 3 Inflammation associated with fungal lesions in both little brown myotis and big brown bats is modified by fungus type. **a** Number of *Pd* lesions plotted against number of inflammatory foci. In little brown myotis (*Myotis lucifugus*; solid black triangles), the number of inflammatory foci was positively associated with number of *Pd* lesions (Pearson's $\rho=0.68$, $p<0.001$), but in big brown bats (*Eptesicus fuscus*; concentric circles), this association was not significant (Pearson's $\rho=0.35$, $p=0.07$). Insets show characteristic *Pd* lesions (black arrows). **b** Number of unidentified fungal invasion foci plotted against the number of inflammatory foci. In both species, number of inflammatory foci was strongly and positively correlated with number of unidentified fungal foci (little brown myotis Pearson's $\rho=0.83$, $p<0.001$, big brown bats Pearson's $\rho=0.82$, $p<0.001$). Grey shading indicates 95% CI around line of best fit. Black bars represent 100 μm

brown myotis: Pearson's $\chi^2 = 32.58$, $p<0.001$; big brown bats: Pearson's $\chi^2 = 9.20$, $p=0.01$) indicating potential fungal proliferation at cold and humid conditions (i.e., the unidentified fungus is psychrophilic or cold tolerant). Amount of the unidentified fungal infection also increased in both species throughout our experiment (little brown myotis Welch's $F_{2,70} = 29.96$, $p<0.001$; big brown bats Welch's $F_{2,53} = 20.29$, $p<0.001$). In both species, the number of observed unidentified fungal foci (and the proportion of wing membrane affected) correlated

positively with the number of observed *Pd* lesions (little brown myotis $n=37$, Pearson's $\rho=0.88$, $p<0.001$, big brown bats $n=28$, Pearson's $\rho=0.42$, $p<0.03$). In both species, the number of inflammatory foci was strongly and positively correlated with the number of unidentified fungal foci (Fig. 3b, little brown myotis $n=73$, Pearson's $\rho=0.83$, $p<0.001$, big brown bats $n=56$, Pearson's $\rho=0.82$, $p<0.001$).

Discussion

Little brown myotis are more susceptible to experimental *Pd* infection than big brown bats, as indicated by higher prevalence and severity of *Pd* infections in this species and by the fact that *Pd* prevalence increased over time in little brown myotis, but not in big brown bats. By the end of the experiment, 13 weeks after inoculation, 100% of little brown myotis were histologically positive for WNS, in contrast to 30% of big brown bats. This finding is in line with field observations of differences in *Pd* prevalence and of mortality (Turner et al. 2011; Langwig et al. 2012, 2015; Frick et al. 2015). We (Reeder and Moore 2013) have previously suggested that free-ranging big brown bats may fare better in response to *Pd*, because they naturally hibernate for a shorter period of time and at colder temperatures (below the optimal *Pd* growth temperature; Verant et al. 2012) than little brown myotis. However, this generalization may not be accurate across populations, as Dunbar and Brigham (2010) found range-wide variation in big brown bat thermoregulatory patterns. Our study was not designed to specifically test for differences in mortality between the two species. However, we found differences in susceptibility after experimentally controlling for environmental factors, which advances our understanding of species variation in disease susceptibility and suggests that bat host physiology plays a role.

One aspect of physiology that may influence disease susceptibility is the thermoregulatory response to *Pd* infection. *Pd*-exposed big brown bats exhibited longer torpor bouts than controls (Fig. 2), a response indicative of greater energy conservation. Because big brown bats exposed to *Pd* aroused from torpid to euthermic temperatures less frequently than controls, they likely retained more of their fat stores (Thomas et al. 1990), though we did not find body condition differences between *Pd*-exposed and control big brown bats. It is possible that torpor duration variability within control and *Pd*-exposed big brown bats, with some individuals in the *Pd*-exposed group showing less dramatic increases in duration, could have resulted in fewer differences in body condition between groups. It is also possible that the duration of our experiment was not sufficiently long to demonstrate energy savings in big brown bats. The potential fat conservation through temperature regulation

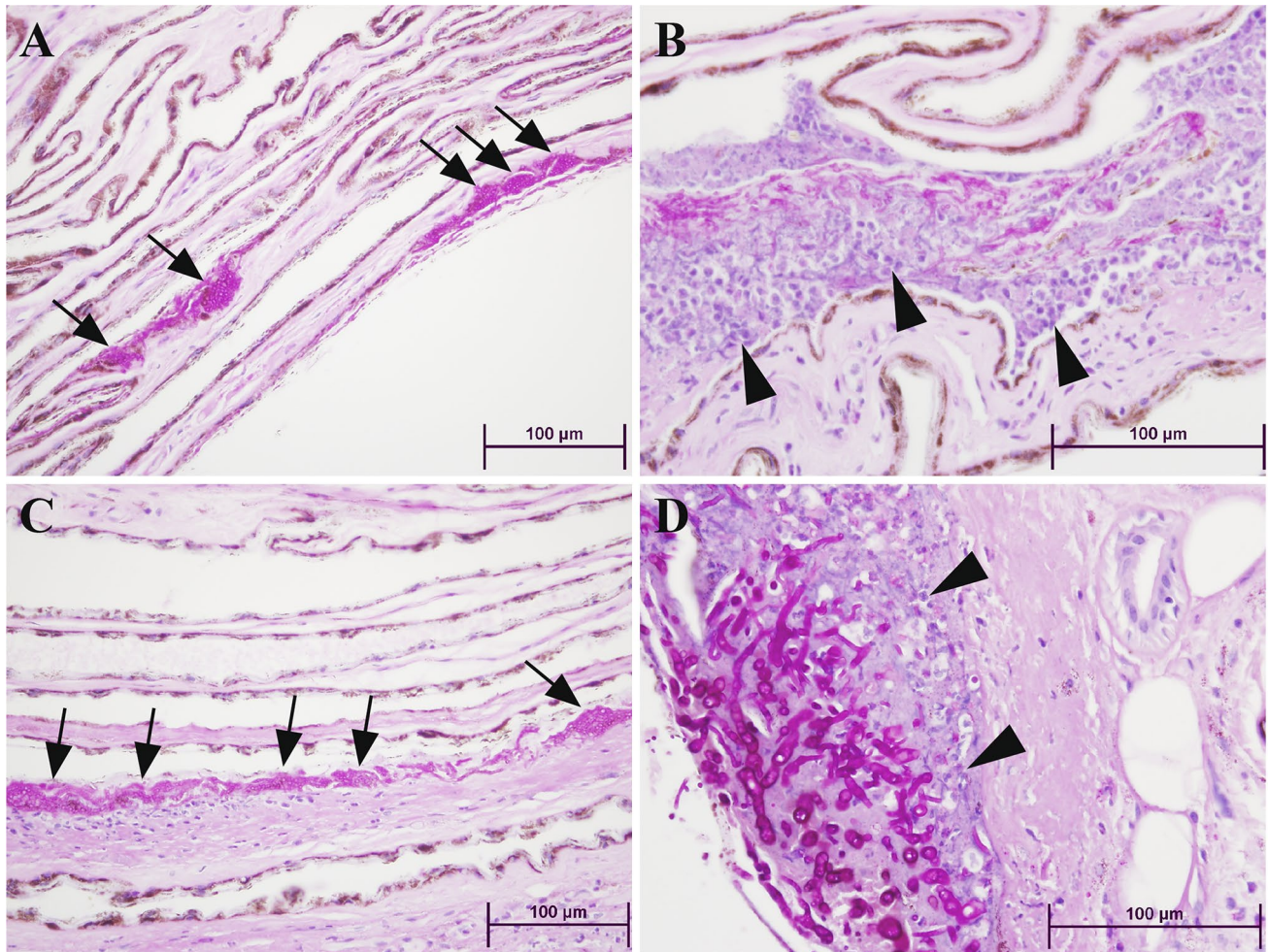


Fig. 4 Histology of skin sections showing *Pseudogymnoascus destructans* (*Pd*) lesions and unidentified infection with associated neutrophilic inflammation in the little brown myotis (*Myotis lucifugus*) and the big brown bat (*Eptesicus fuscus*). **a** Characteristic *Pd* lesions (long black arrows) in the epidermis and superficial dermis of a little brown myotis. Tightly packed, PAS-positive, magenta-colored fungal hyphae form cupping erosions. Cross-sections of hyphae have a bubbly appearance. **b** Unidentified fungal invasion with associated neutrophilic inflammation (blunt arrows) in a hibernating little brown myotis. Very slender, septate hyphae with bulbous

dilations are found in large numbers in the exudate. **c** Characteristic *Pd* lesions (long black arrows) in epidermis and superficial dermis of a big brown bat. Cupping erosions are less distinct and more confluent than in little brown myotis, but tightly packed hyphae have the bubbly appearance of *Pd*. **d** Unidentified fungal invasion associated with epidermal ulceration, dermal necrosis, and inflammation (blunt arrows) in a hibernating big brown bat. Variably sized, but generally quite large, globose, septate hyphae show non-dichotomous branching. Periodic acid-Schiff stain. (Color figure online)

over the course of a full hibernation season could provide big brown bats with the ability to mount a more effective anti-*Pd* immune response and not expend energy stores to their limit. The previous studies using other methods have demonstrated altered immune parameters in WNS-affected little brown myotis, suggesting a costly but ineffective immune response to *Pd* (Moore et al. 2011, 2013; Field et al. 2015; Johnson et al. 2015; Lilley et al. 2017). Further study will be needed to determine if *Pd* infection of big brown bats produces a different type of and/or less robust immune response than in little brown myotis. We did not detect significantly altered thermoregulation

patterns in *Pd*-exposed little brown myotis. The previous field and captive studies have clearly established that little brown myotis demonstrate maladaptive thermoregulatory shifts during WNS, especially towards the end of hibernation (Reeder et al. 2012; Warnecke et al. 2012; Johnson et al. 2014). However, not all experimental studies have found statistically significant differences in torpor dynamics between *Pd*-exposed and uninfected bats (Verant et al. 2014; Brownlee-Bouboulis and Reeder 2013), suggesting that experimental studies do not perfectly replicate natural infections, which are typically of longer duration (Reeder et al. 2012, 2016; Field et al. 2015).

We observed a significant inflammation in the wing tissues of both little brown myotis and big brown bats. The previous studies, based on wild-sampled bats, generally found little to no histological evidence of inflammation in tissues of hibernating WNS-affected bats (Meteyer et al. 2009; Cryan et al. 2010), except for one report consistent with immune response inflammatory syndrome in bats after emergence from hibernation in spring (Meteyer et al. 2012). We exposed bats to a pure isolate of *Pd*; however, 69.7% of *Pd*-exposed bats and 67.2% of controls showed histological evidence of a fungal infection not morphologically similar to *Pd*. More big brown bats exhibited the unidentified fungal infection compared with little brown myotis, but the unidentified fungal infection was particularly severe in *Pd*-exposed little brown myotis. Control little brown myotis with lower measures of body condition when we collected them in the wild were also particularly susceptible to the unidentified fungal infection. In both species, the unidentified fungal infection increased in prevalence and severity over the course of our experiment, suggesting this fungus (or fungi) is psychrophilic, or at least cold tolerant. Inflammation also increased over the course of our experiment and was strongly correlated with colonization by the unidentified fungus (or fungi) in both species, but correlated, although less strongly, with severity of *Pd* infection only in little brown myotis. We interpret this to mean that the inflammation observed might be due to colonization by the unidentified fungus (or fungi) and not by *Pd*. In a separate study, Field et al. (2015) found that *Pd*-infected little brown myotis significantly up-regulated the expression of inflammation-inducing genes but that, despite the apparent production of appropriate chemokines, immune cells such as neutrophils and T cells do not appear to be recruited. While it is possible that intralesional bacteria contributed to the observed inflammation (Meteyer et al. 2009), we did not detect any consistent intralesional bacteria associated with inflammation in this study. Especially in light of WNS, it is important to note that hibernating little brown myotis and big brown bats are capable of inflammatory responses in the skin in association with fungal invasion, but not in response specifically to *Pd*. Because many fungal pathogens demonstrate immune evasion (Chai et al. 2009), future studies focused on the pathogenesis of *Pd* should investigate mechanisms underlying evasion of host immune responses.

Our results clearly support the hypothesis that when held under identical conditions and exposed to the same inoculation dose of *Pd*, big brown bats are less susceptible to *Pd* infection than little brown myotis. Big brown bats developed fewer and less severe infections than little brown myotis. Despite their lower infection rate, lower number of lesions when infected, and qualitatively “less defined” lesions with more confluent foci, big brown bats significantly increased the time spent in torpor when

infected with *Pd*. This adaptive energetic response is in direct contrast to the energy-consuming decrease in torpor bout length for little brown myotis (Reeder et al. 2012; Warnecke et al. 2012; Johnson et al. 2014). These differences likely influence disease progression as the thermoregulatory response to infection in big brown bats is consistent with greater resistance to WNS in this species.

The degree to which our results from these two relatively common and relatively well-studied ‘model’ bat species apply to other rare or otherwise poorly studied species is unknown (Reeder et al. 2016; Hayman et al. 2016), but our study provides an important starting point. From our findings of differential thermoregulatory responses between species, we can infer that the thermoenergetic response to infection will play a major role in determining disease progression in other hibernating species. In addition, numerous other species-specific factors, including life history traits, metabolic and immune responses to *Pd* infection, and variability in the dynamics of host–pathogen interactions likely contribute to differential susceptibility (Reeder and Moore 2013; Hayman et al. 2016). The species-specific nature of the thermoregulatory response to *Pd* infection in our study is striking in that it did not differ in degree but rather in direction. This suggests that the increased arousals from hibernation in response to *Pd* infection, which have been considered a hallmark of WNS pathology that directly contribute to fat store loss and mortality, are not ubiquitous. For big brown bats, Hayman et al. (2016) modelled thermoregulatory parameters that would affect mortality in the face of *Pd* infection. Our empirical findings are in support of this model, in which increased torpor duration was associated with less severe infection.

The physiological underpinnings of this contrasting response to *Pd* infection in this WNS-resistant bat species are unknown, but they are presumably mediated by immune and metabolic processes and moderated by host–pathogen interactions. Whether other species that display resistance to *Pd* infection share the same response profile as big brown bats and likewise, whether other highly susceptible species display a similar response profile to that of little brown bats remains to be studied.

Acknowledgements This study was supported by the United States Fish and Wildlife Service (F11AP00073 to DMR) and the National Science Foundation (DEB-1115895 to WFF and JTF). MSM was partially supported by the National Institute of General Medicine Sciences of the National Institutes of Health (K12GM102778). We thank Cindy Rhone and Gretchen Long for animal care assistance and Kevin Keel for providing *P. destructans* isolate used for inoculations.

Compliance with ethical standards

Conflict of interest The authors declare that they have no conflict of interest.

Ethical approval All applicable international, national, and/or institutional guidelines for the care and use of animals were followed. All procedures performed in studies involving animals were in accordance with the ethical standards of Bucknell University (see “Materials and methods” for further description).

References

- Avena CV, Parfrey LW, Leff JW, Archer HM, Frick WF, Langwig KE, Kilpatrick AM, Powers KE, Foster JT, McKenzie VJ (2016) Deconstructing the bat skin microbiome: influences of the host and the environment. *Front Microbiol* 7:1753
- Benjamini Y, Hochberg Y (1995) Controlling the false discovery rate—a practical and powerful approach to multiple testing. *J Roy Stat Soc B Met* 57:289–300
- Bernard RF, Foster JT, Willcox EV, Parise KL, McCracken GF (2015) Molecular detection of the causative agent of white-nose syndrome on Rafinesque’s big-eared bats (*Corynorhinus rafinesquii*) and two species of migratory bats in the southeastern USA. *J Wildlife Dis* 51:519–522
- Blehert DS, Hicks AC, Behr M, Meteyer CU, Berlowski-Zier BM, Buckles EL, Coleman JT, Darling SR, Gargas A, Niver R et al (2009) Bat white-nose syndrome: an emerging fungal pathogen? *Science* 323:227
- Brownlee-Bouboulis SA, Reeder DM (2013) White-nose syndrome-affected little brown myotis (*Myotis lucifugus*) increase grooming and other active behaviors during arousals from hibernation. *J Wildlife Dis* 49:850–859
- Chai LY, Netea MG, Vonk AG, Kullberg BJ (2009) Fungal strategies for overcoming host innate immune response. *Med Mycol* 47:227–236
- Chaturvedi V, Springer DJ, Behr MJ, Ramani R, Li X, Peck MK, Ren P, Bopp DJ, Wood B, Samsonoff WA, Butchkoski CM (2010) Morphological and molecular characterizations of psychrophilic fungus *Geomyces destructans* from New York bats with white nose syndrome (WNS). *PLoS One* 5:e10783
- Courtin F, Stone WB, Risatti G, Gilbert K, Van Kruiningen HJ (2010) Pathogenic findings and liver elements in hibernating bats with white-nose syndrome. *Vet Pathol* 47:214–219
- Cryan PM, Meteyer CU, Boyles JG, Blehert DS (2010) Wing pathology of white-nose syndrome in bats suggests life-threatening disruption of physiology. *BMC Biol* 8:135
- Dobson A, Fofopoulos J (2001) Emerging infectious pathogens of wildlife. *Philos Trans R Soc Lond B Biol Sci* 356:1001–1012
- Dunbar MB, Brigham RM (2010) Thermoregulatory variation among populations of bats along a latitudinal gradient. *J Comp Phys B* 180:885–893
- Field KA, Johnson JS, Lilley TM, Reeder SM, Rogers EJ, Behr MJ, Reeder DM (2015) The white-nose syndrome transcriptome: activation of anti-fungal host responses in wing tissue of hibernating little brown myotis. *PLoS Pathog* 11:e1005168
- Francl KE, Sparks DW, Brack V, Timponi J (2011) White-nose syndrome and wing damage index scores among summer bats in the northeastern United States. *J Wildlife Dis* 47:41–48
- Frank CL, Michalski A, McDonough AA, Rahimian M, Rudd RJ, Herzog C (2014) The resistance of a North American bat species (*Eptesicus fuscus*) to white-nose syndrome (WNS). *PLoS One* 9:e113958
- Frank CL, Ingala MR, Ravenelle RE, Dougherty-Howard K, Wicks SO, Herzog C, Rudd RJ (2016) The effects of cutaneous fatty acids on the growth of *Pseudogymnoascus destructans*, the etiological agent of white-nose syndrome (WNS). *PLoS One* 11:e0153535
- Frick WF, Pollock JF, Hicks AC, Langwig KE, Reynolds DS, Turner GG, Butchkoski CM, Kunz TH (2010) An emerging disease causes regional population collapse of a common North American bat species. *Science* 329:679–682
- Frick WF, Puechmaile SJ, Hoyt JR, Nickel BA, Langwig KE, Foster JT, Barlow KE, Bartonička T, Feller D, Haarsma AJ (2015) Disease alters macroecological patterns of North American bats. *Global Ecol Biogeogr* 24:741–749
- Fuller NW, Reichard JD, Nabhan ML, Fellows SR, Pepin LC, Kunz TH (2011) Free-ranging little brown myotis (*Myotis lucifugus*) heal from wing damage associated with white-nose syndrome. *Ecohealth* 8:154–162
- Gargas A, Trest MT, Christensen M, Volk TJ, Blehert DS (2009) *Geomyces destructans* sp nov associated with bat white-nose syndrome. *Mycotaxon* 108:147–154
- Grieneisen LE, Brownlee-Bouboulis SA, Johnson JS, Reeder DM (2015) Sex and hibernaculum temperature predict survivorship in white-nose syndrome affected little brown myotis (*Myotis lucifugus*). *R Soc Open Sci* 2:140470
- Hallsall AL, Boyles JG, Whitaker JO (2012) Body temperature patterns of big brown bats during winter in a building hibernaculum. *J Mammal* 93:497–503
- Hayman DTS, Pulliam JRC, Marshall JC, Cryan PM, Webb CT (2016) Environment, host, and fungal traits predict continental-scale white-nose syndrome in bats. *Sci Adv* 2:e1500831
- Hoyt JR, Cheng TL, Langwig KE, Hee MM, Frick WF, Kilpatrick AM (2015) Bacteria isolated from bats inhibit the growth of *Pseudogymnoascus destructans*, the causative agent of white-nose syndrome. *PLoS One* 10:e0121329
- Hoyt JR, Sun K, Parise KL, Lu G, Langwig KE, Jiang T, Yang S, Frick WF, Kilpatrick AM, Foster JT, Feng J (2016) Widespread bat white-nose syndrome fungus, northeastern China. *Emerg Infect Dis* 22:140–142
- Johnson JS, Reeder DM, McMichael JW 3rd, Meierhofer MB, Stern DW, Lumadue SS, Sigler LE, Winters HD, Vozzak ME, Kurta A et al (2014) Host, pathogen, and environmental characteristics predict white-nose syndrome mortality in captive little brown myotis (*Myotis lucifugus*). *PLoS One* 9:e112502
- Johnson JS, Reeder DM, Lilley TM, Czirájk GÁ, Voigt CC, McMichael JW 3rd, Meierhofer MB, Seery CW, Lumadue SS, Altmann AJ et al (2015) Antibodies to *Pseudogymnoascus destructans* are not sufficient for protection against white-nose syndrome. *Ecol Evol* 5:2203–2214
- Langwig KE, Frick WF, Bried JT, Hicks AC, Kunz TH, Kilpatrick AM (2012) Sociality, density-dependence and microclimates determine the persistence of populations suffering from a novel fungal disease, white-nose syndrome. *Ecol Lett* 15:1050–1057
- Langwig KE, Frick WF, Reynolds R, Parise KL, Drees KP, Hoyt JR, Cheng TL, Kunz TH, Foster JT, Kilpatrick AM (2015) Host and pathogen ecology drive the seasonal dynamics of a fungal disease, white-nose syndrome. *Proc Roy Soc Lond B: Biol Sci* 282:20142335
- Leopardi S, Blake D, Puechmaile SJ (2015) White-nose syndrome fungus introduced from Europe to North America. *Curr Biol* 25:R217–R219
- Lilley TM, Prokko JM, Johnson JS, Rogers EJ, Gronsky S, Kurta A, Reeder DM, Field KA (2017) Immune responses in hibernating little brown myotis (*Myotis lucifugus*) with white-nose syndrome. *Proc Roy Soc Lond B: Biol Sci*. doi:10.1098/rspb.2016.2232
- Lorch JM, Meteyer CU, Behr MJ, Boyles JG, Cryan PM, Hicks AC, Ballmann AE, Coleman JT, Redell DN, Reeder DM et al (2011) Experimental infection of bats with *Geomyces destructans* causes white-nose syndrome. *Nature* 480:376–378
- Meteyer CU, Buckles EL, Blehert DS, Hicks AC, Green DE, Shearn-Bochsler V, Thomas NJ, Gargas A, Behr MJ (2009)

- Histopathologic criteria to confirm white-nose syndrome in bats. *J Vet Diagn Invest* 21:411–414
- Meteyer CU, Barber D, Mandl JN (2012) Pathology in euthermic bats with white nose syndrome suggests a natural manifestation of immune reconstitution inflammatory syndrome. *Virulence* 3:583–588
- Moore MS, Reichard JD, Murtha TD, Zahedi B, Fallier RM, Kunz TH (2011) Specific alterations in complement protein activity of little brown myotis (*Myotis lucifugus*) hibernating in white-nose syndrome affected sites. *PLoS One* 6:e27430
- Moore MS, Reichard JD, Murtha TD, Nabhan ML, Pian RE, Ferreira JS, Kunz TH (2013) Hibernating little brown myotis (*Myotis lucifugus*) show variable immunological responses to white-nose syndrome. *PLoS One* 8:e58976
- Muller LK, Lorch JM, Lindner DL, O'Connor M, Gargas A, Blehert DS (2013) Bat white-nose syndrome: a real-time TaqMan polymerase chain reaction test targeting the intergenic spacer region of *Geomyces destructans*. *Mycologia* 105:253–259
- Pikula J, Bandouchova H, Novotný L, Meteyer CU, Zukal J, Irwin NR, Zima J, Martinkova N (2011) Histopathology confirms white-nose syndrome in bats in Europe. *J Wildlife Dis* 48:207–211
- Puechmaile SJ, Wibbelt G, Korn V, Fuller H, Forget F, Mühldorfer AK, Bogdanowicz W, Borel C, Bosch T, Cherezy T et al (2011) Pan-European distribution of white-nose syndrome fungus (*Geomyces destructans*) not associated with mass mortality. *PLoS One* 6:e19167
- Reeder DM, Moore MS (2013) White-nose syndrome: a deadly emerging infectious disease of hibernating bats. In: Adams RA, Pederson SC (eds) *Bat evolution, ecology, and conservation*. Springer, New York, pp 413–434
- Reeder DM, Frank CL, Turner GG, Meteyer CU, Kurta A, Britzke ER, Vodzak ME, Darling SR, Stihler CW, Hicks AC et al (2012) Frequent arousal from hibernation linked to severity of infection and mortality in bats with white-nose syndrome. *PLoS One* 7:e38920
- Reeder DM, Field KA, Slater MH (2016) Balancing the costs of wildlife research with the benefits of understanding a panzootic disease, white-nose syndrome. *The Institute for Laboratory Animal Research (ILAR) Journal* 56:275–282
- Reichard JD, Kunz TH (2009) White-nose syndrome inflicts lasting injuries to the wings of little brown myotis (*Myotis lucifugus*). *Acta Chiropterol* 11:457–464
- Romani L (2011) Immunity to fungal infections. *Nat Rev Immunol* 11:275–288
- Skerratt LF, Berger L, Speare R, Cashins S, McDonald KR, Phillott AD, Hines HB, Kenyon N (2007) Spread of chytridiomycosis has caused the rapid global decline and extinction of frogs. *EcoHealth* 4:125–134
- Storm JJ, Boyles JG (2011) Body temperature and body mass of hibernating little brown bats *Myotis lucifugus* in hibernacula affected by white-nose syndrome. *Acta Theriol* 56:123–127
- Thogmartin WE, King RA, McKann PC, Szymanski JA, Pruitt L (2012) Population-level impact of white-nose syndrome on the endangered Indiana bat. *J Mammal* 93:1086–1098
- Thogmartin WE, Sanders-Reed CA, Szymanski JA, McKann PC, Pruitt L, King RA, Runge MC, Russell RE (2013) White-nose syndrome is likely to extirpate the endangered Indiana bat over large parts of its range. *Biol Conserv* 160:162–172
- Thomas DW, Dorais M, Bergeron J-M (1990) Winter energy budgets and cost of arousals for hibernating little brown bats, *Myotis lucifugus*. *J Mammal* 71:475–479
- Tompkins DM, Carver S, Jones ME, Krkošek M, Skerratt LF (2015) Emerging infectious diseases of wildlife: a critical perspective. *Trends Parasitol* 31:149–159
- Turner GG, Reeder DM, Coleman JTH (2011) A five-year assessment of mortality and geographic spread of white-nose syndrome in North American bats and a look to the future. *Bat Res News* 52:13–27
- Turner GG, Meteyer CU, Barton H, Gumbs JF, Reeder DM, Overton B, Bandouchova H, Bartonicka T, Martinkova N, Pikula J et al (2014) Nonlethal screening of bat-wing skin with the use of ultraviolet fluorescence to detect lesions indicative of white-nose syndrome. *J Wildlife Dis* 50:566–573
- USFWS (2012) News Release: North American bat death toll exceeds 5.5 million from white-nose syndrome. http://www.fws.gov/whitenosesyndrome/pdf/WNS_Mortality_2012_NR_FINAL.pdf. Accessed 4 May 2012
- Verant ML, Boyles JG, Waldrep W Jr, Wibbelt G, Blehert DS (2012) Temperature-dependent growth of *Geomyces destructans*, the fungus that causes bat white-nose syndrome. *PLoS One* 7:e46280
- Verant ML, Meteyer CU, Speakman JR, Cryan PM, Lorch JM, Blehert DS (2014) White-nose syndrome initiates a cascade of physiological disturbances in the hibernating bat host. *BMC Physiol* 14:10
- Warnecke L, Turner JM, Bollinger TK, Lorch JM, Misra V, Cryan PM, Wibbelt G, Blehert DS, Willis CKR (2012) Inoculation of bats with European *Geomyces destructans* supports the novel pathogen hypothesis for the origin of white-nose syndrome. *Proc Natl Acad Sci USA* 109:6999–7003
- Warnecke L, Turner JM, Bollinger TK, Misra V, Cryan PM, Blehert DS, Wibbelt G, Willis CKR (2013) Pathophysiology of white-nose syndrome in bats: a mechanistic model linking wing damage to mortality. *Biol Lett* 9:20130177
- Wickham H (2009) *ggplot2: elegant graphics for data analysis*. Springer, New York
- Wilcox A, Warnecke L, Turner JM, McGuire LP, Jameson JW, Misra V, Bollinger TC, Willis CKR (2014) Behaviour of hibernating little brown bats experimentally inoculated with the pathogen that causes white-nose syndrome. *Anim Behav* 88:157–164
- Wilder AP, Frick WF, Langwig KE, Kunz TH (2011) Risk factors associated with mortality from white-nose syndrome among hibernating bat colonies. *Biol Lett* 7:950–953
- Willis CKR, Brigham RM (2003) Defining torpor in free-ranging bats: experimental evaluation of external temperature-sensitive radiotransmitters and the concept of active temperature. *J Comp Physiol B* 173:379–389
- Willis CKR, Menzies AK, Boyles JG, Wojciechowski MS (2011) Evaporative water loss is a plausible explanation for mortality of bats from white-nose syndrome. *Integr Comp Biol* 51:364–373
- Zukal J, Bandouchova H, Bartonicka T, Berkova H, Brack V, Brichta J, Dolinay M, Jaron KS, Kovacova V, Kovarik M et al (2014) White-nose syndrome fungus: a generalist pathogen of hibernating bats. *PLoS One* 9:e97224